J Appl Physiol 93: 1939–1946, 2002.
First published August 23, 2002; 10.1152/japplphysiol.00544.2002.

Stent implantation alters coronary artery hemodynamics and wall shear stress during maximal vasodilation

JOHN F. LADISA JR.,[1,2] DOUGLAS A. HETTRICK,[1,2] LARS E. OLSON,[2] ISMAIL GULER,[3] ERIC R. GROSS,[1] TOBIAS T. KRESS,[1] JUDY R. KERSTEN,[1,4] DAVID C. WARLTIER,[1,2,4,5] AND PAUL S. PAGEL[1,2,4]

[1]*Departments of Anesthesiology,* [5]*Medicine (Division of Cardiovascular Diseases), and* [4]*Pharmacology and Toxicology, Medical College of Wisconsin and the Clement J. Zablocki Veterans Affairs Medical Center, Milwaukee 53226; and* [2]*Department of Biomedical Engineering, Marquette University, Milwaukee, Wisconsin 53201; and* [3]*Boston Scientific-SciMed, Maple Grove, Minnesota 55311*

Received 21 June 2002; accepted in final form 20 August 2002

LaDisa Jr., John F., Douglas A. Hettrick, Lars E. Olson, Ismail Guler, Eric R. Gross, Tobias T. Kress, Judy R. Kersten, David C. Warltier, and Paul S. Pagel. Stent implantation alters coronary artery hemodynamics and wall shear stress during maximal vasodilation. *J Appl Physiol* 93: 1939–1946, 2002. First published August 23, 2002; 10.1152/japplphysiol.00544.2002.—Coronary stents improve resting blood flow and flow reserve in the presence of stenoses, but the impact of these devices on fluid dynamics during profound vasodilation is largely unknown. We tested the hypothesis that stent implantation affects adenosine-induced alterations in coronary hemodynamics and wall shear stress in anesthetized dogs ($n = 6$) instrumented for measurement of left anterior descending coronary artery (LAD) blood flow, velocity, diameter, and radius of curvature. Indexes of fluid dynamics and shear stress were determined before and after placement of a slotted-tube stent in the absence and presence of an adenosine infusion (1.0 mg/min). Adenosine increased blood flow, Reynolds (Re) and Dean numbers (De), and regional and oscillatory shear stress concomitant with reductions in LAD vascular resistance and segmental compliance before stent implantation. Increases in LAD blood flow, Re, De, and indexes of shear stress were observed after stent deployment ($P < 0.05$). Stent implantation reduced LAD segmental compliance to zero and potentiated increases in segmental and coronary vascular resistance during adenosine. Adenosine-induced increases in coronary blood flow and reserve, Re, De, and regional and oscillatory shear stress were attenuated after the stent was implanted. The results indicate that stent implantation blunts alterations in fluid dynamics during coronary vasodilation in vivo.

slotted-tube endovascular stents; coronary impedance; coronary artery disease

ENDOVASCULAR STENTS ARE ROUTINELY implanted to improve or restore distal perfusion in patients with coronary artery and peripheral vascular disease. Unfortunately, neointimal hyperplasia occurs in 15–20% of these patients (10, 27, 28). Alterations in coronary hemodynamics and vascular injury produced by stent deployment within the stented region may contribute to restenosis after stent placement. Stent geometry may affect coronary flow reserve (29) and produce reductions in wall shear stress and resistance after implantation. Whether alterations in resistance and temporal wall shear stress distributions occur during coronary vasodilation after stent implantation is presently unknown. Identification of the hemodynamic factors that may contribute to restenosis may lead to improved stent design and application. Thus we tested the hypothesis that stent implantation alters the actions of the coronary vasodilator, adenosine, on coronary fluid dynamics and temporal wall shear stress in anesthetized dogs.

MATERIALS AND METHODS

All experimental procedures and protocols used in this investigation were reviewed and approved by the Animal Care and Use Committee of the Medical College of Wisconsin and Marquette University. All conformed to the "Guide for the Care and Use of Laboratory Animals" (Office of Science and Health Reports, DRR/NIH, Bethesda, MD 20205).

Surgical preparation. Adult mongrel dogs ($n = 6$) of either sex, weighing between 25 and 30 kg, were fasted overnight, anesthetized with pentobarbital sodium (25 mg/kg) and barbital (200 mg/kg), and ventilated by using positive pressure with a mixture of oxygen (28–30%) and air after tracheal intubation. Respiratory rate and tidal volume were adjusted to maintain arterial blood pH and the P_{CO_2} within physiological limits. Fluid deficits were replaced before experimentation with 500 ml of 0.9% saline, which was continued at 3 $ml \cdot kg^{-1} \cdot h^{-1}$ for the duration of each experiment. Fluid-filled catheters were inserted into the right femoral vein and artery for fluid administration and arterial blood-gas sampling, respectively. A thoracotomy was performed in the fifth intercostal space, the lungs gently retracted, and the pericardium opened.

Left ventricular and coronary artery instrumentation. The instrumentation used to assess alterations in coronary and systemic hemodynamics is illustrated in Fig. 1 and was

Address for reprint requests and other correspondence: P. S. Pagel, Medical College of Wisconsin, MEB-M4280, 8701 Watertown Plank Rd., Milwaukee, WI 53226 (E-mail: pspagel@mcw.edu).

The costs of publication of this article were defrayed in part by the payment of page charges. The article must therefore be hereby marked "*advertisement*" in accordance with 18 U.S.C. Section 1734 solely to indicate this fact.

consistent across all interventions and experiments. A 7-Fr, dual-micromanometer-tipped catheter (Millar) was inserted into the left ventricle (LV) and ascending aorta for measurement of LV and arterial pressures, respectively. Transit-time (Transonic) and Doppler flow probes were placed around the proximal left anterior descending coronary artery (LAD) for measurement of blood flow and local blood flow velocity proximal to the stent inlet, respectively. A second Doppler flow probe was positioned ~16 mm distal to the proximal probe for measurement of local velocity at the outlet of the deployed stent. A silk ligature was placed around a small distal branch of the LAD for subsequent use in stent placement. A 2.5-mm ultrasonic segment length transducer (Triton) was placed around the LAD for measurement of continuous external coronary artery diameter. A pair of ultrasonic segment length transducers was positioned on the epicardial surface of the LAD perfusion territory for measurement of diameter of curvature of the LV free wall. A fluid-filled catheter was inserted into the left atrium through the atrial appendage for administration of adenosine. Hemodynamic data were digitally recorded (364 Hz) by using a computer interfaced with an analog-to-digital converter.

Experimental protocol. Intravenous heparin (100 IU/kg) was administered at the completion of the surgical preparation (26). Baseline systemic and coronary hemodynamics were recorded 30 min after completion of instrumentation. Adenosine was infused (1.0 mg/min) by using the left atrial catheter to achieve maximum LAD vasodilation, as assessed by a sevenfold increase in diastolic coronary blood flow (31), and hemodynamics were recorded under steady-state conditions after a 20-min equilibration period. The adenosine infusion was then discontinued, and hemodynamics were allowed to return to baseline values. A 2.5 × 16 mm slotted-tube stent was positioned between the two Doppler flow velocity probes by using the small distal arterial branch of the LAD that had been snared during the surgical preparation. The stent was deployed by using a stent-to-artery size ratio of 1.1–1.2:1 (11). The distal LAD branch was then resnared after the stent had been successfully deployed. Hemodynamics were recorded 30 min after the stent had been placed, and the adenosine infusion was repeated by using the methods described above. Each dog was euthanized with an overdose of pentobarbital sodium after completion of the experiment, and the position of all instruments and the stent was confirmed.

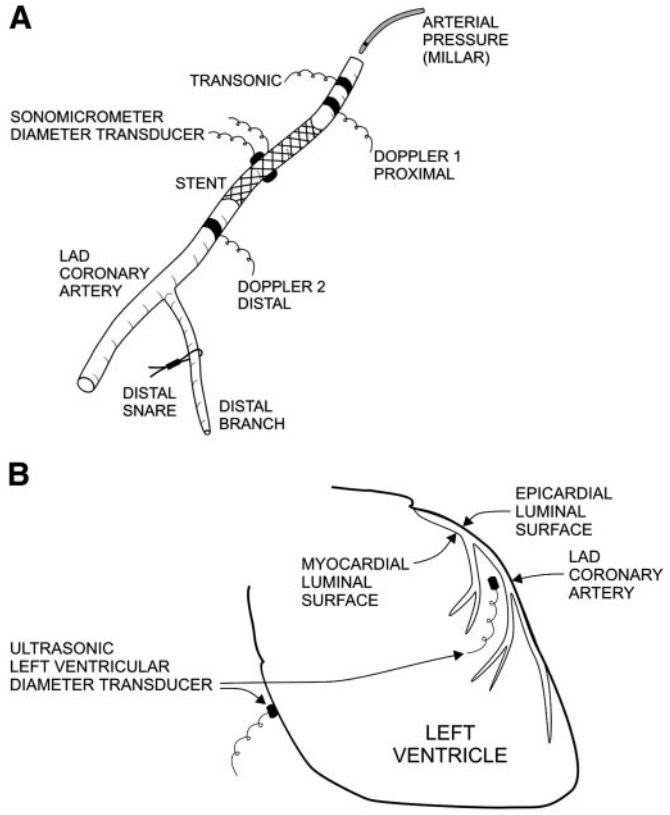

Fig. 1. *A*: schematic diagram of the instrumentation utilized to determine arterial pressure, left anterior descending coronary artery (LAD) regional and local blood flow velocity, external vessel diameter, and the site of stent implantation. *B*: the location of the epicardial and myocardial luminal surfaces and the ultrasonic segment length transducers used to determine the diameter of curvature of the left ventricular (LV) free wall in the LAD perfusion territory.

Ensemble averaging of hemodynamics. LV and aortic blood pressure, LAD blood flow, proximal and distal LAD blood velocity, LAD external diameter, and LAD diameter of curvature waveforms were digitally recorded at end expiration for each intervention. A representative time series of one cardiac cycle for each waveform (Fig. 2) was generated by using a custom-designed (Matlab, Mathworks, Natick, MA) program that referenced peak LV pressure to spatially align the variables in each digitized waveform, segment each variable time series, and ensemble average the segments.

Determination of blood viscosity. Blood viscosity (μ) during each intervention was measured in duplicate at 37°C for six different shear rates (15, 30, 56.25, 75, 187.5, and 375 s^{-1}) by using a cone and plate viscometer (DVII$^+$, Brookfield Engineering Labs, Stoughton, MA). The μ was then plotted against shear rate, and relations describing a three-constant exponential decay relationship of the curve were obtained for each intervention by using Marquardt-Levenberg algorithm with commercially available software (Sigma Plot 2000, SPSS, Chicago, IL).

Calculation of indexes of coronary fluid dynamics. The internal LAD radius (r_i) was determined by using the equation $r_i = (r_o^2 - V/L\pi)^{1/2}$, where r_o^2 is the external LAD radius, L is the length between proximal and distal Doppler flow velocity probes in situ, and V is the ratio of the excised vessel weight to density (assumed as 1.06 g/ml) (22). Reynolds number (Re) describes the ratio of convective inertial forces to shear forces in a cylinder and was calculated by using equation $Re = 2r_i \cdot \rho \cdot \bar{v}/\mu$, where ρ is the blood density (1.06 g/ml) and $\bar{v}$ is the temporal mean of the coronary blood flow velocity. Dean number (De) considers the effects of coronary artery curvature on the axial velocity profile and secondary flow and was determined as $De = (2\delta)^{1/2} \cdot 4\ Re$, where δ is the ratio of LAD r_i to the radius of curvature (15). The Womersley number (α) characterizes the ratio of oscillatory inertial forces to shear forces and was estimated as the product of LAD r_i and the square root of the ratio of angular frequency to μ (15). Secondary Re (Re_s) considers the combined actions of LAD pulsatility and curvature and was approximated as $(De/4\alpha)^2$ (19). Regional shear rate (γ) was estimated from coronary blood flow rate ($\dot{Q}$) and r_i by using the equation $\gamma = 4\ \dot{Q}/\pi r_i^3$ and refers to the temporally varying shear rate on the walls of the epicardial LAD. Mean and diastolic coronary vascular resistances were calculated as the ratios of mean and diastolic arterial pressures to mean and diastolic coronary blood flows, respectively. Coronary flow reserve was estimated as the ratio of maximum blood flow during vasodilation to resting flow (24). LAD segmental compliance (C) in the region designated for stent implantation was determined as $C = \pi(dD) \cdot d \cdot L/2dP$, where dD and d are the change

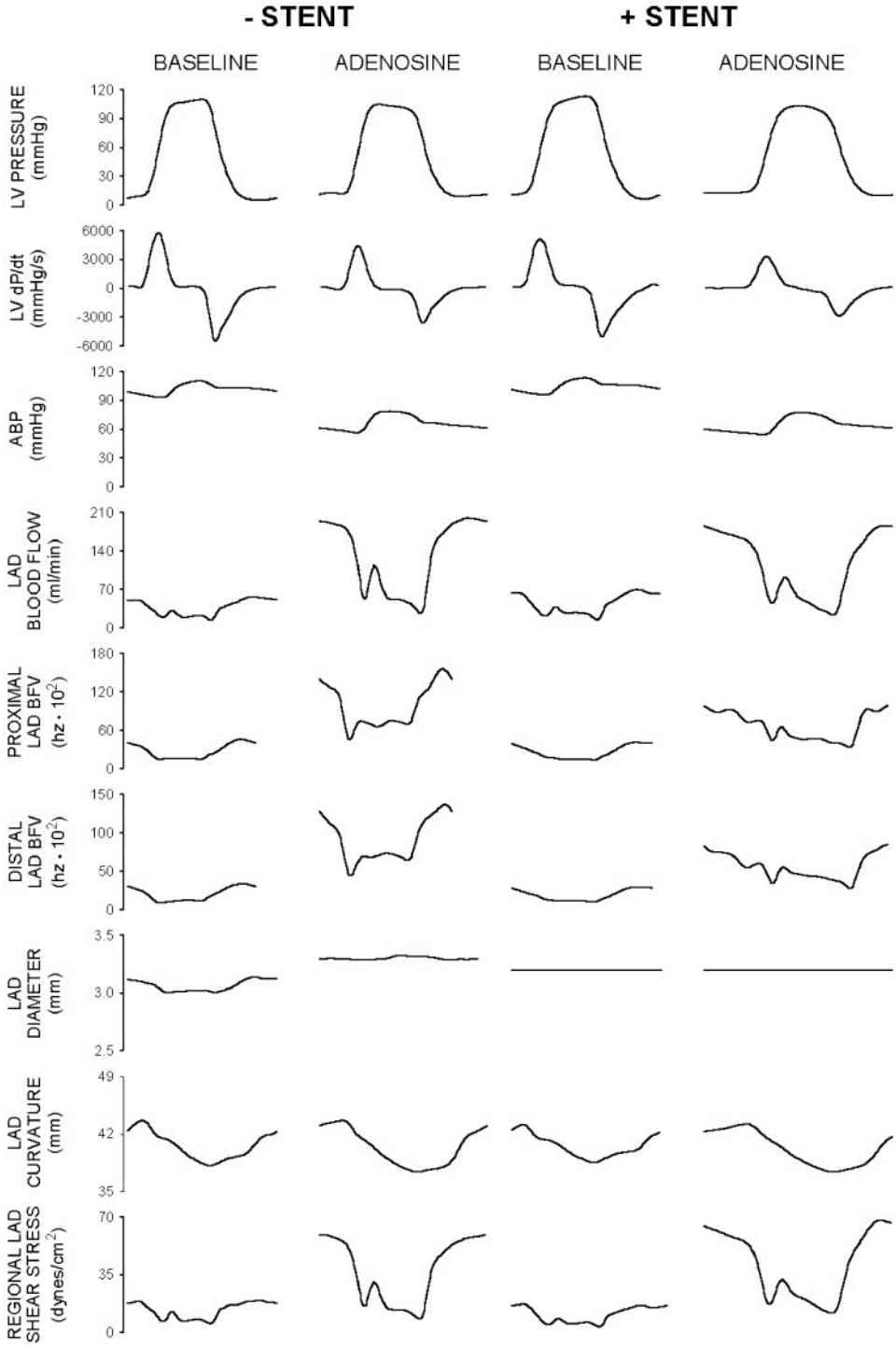

Fig. 2. Ensemble-averaged, single cardiac cycle LV pressure, maximum rate of increase of LV pressure (dP/dt), aortic blood pressure (ABP), LAD blood flow, proximal and distal LAD blood flow velocity (BFV), LAD external diameter, LAD diameter of curvature, and regional LAD shear stress waveforms obtained under baseline conditions and during the administration of adenosine (1.0 mg/min) in the absence (−stent) and presence (+stent) of the intracoronary stent obtained in a typical experiment.

and maximum internal diameter, respectively, of the LAD, dP is the change in arterial pressure during diastole, and L is the length of the deployed stent (17). Additionally, Poiseuillean resistance (PR) in the stented region was calculated as $PR = 8\mu L/\pi r_i^4$.

Estimation of local blood flow velocity and shear rate. Local blood flow velocity was determined 1–3 mm proximal and distal to the implanted stent at the epicardial and myocardial luminal surfaces of the LAD. Doppler pulse penetration depth was monitored by digital readout of the Doppler module adjustable focus depth. Digitized sample volumes (~0.23 mm^3) were obtained at a minimum of 14 axial depths across the vessel and converted to velocity by using the equation $\nu = 2\Delta fc/f_o \cos\theta$, where ν is the blood velocity, Δf is the Doppler frequency shift, f_o is the initial frequency of the ultrasonic pulse, c is the wave speed, and θ is the piezoelectric crystal insonation angle (1). Doppler penetration depths rendering zero blood flow were assumed to be indicative of the epicardial and myocardial luminal surfaces. Velocity waveforms at each axial depth were ensemble averaged (Fig. 3*A*) and spatially aligned to reconstruct velocity profiles (Fig. 3*B*) for each intervention. Least squared interpolation was then per-

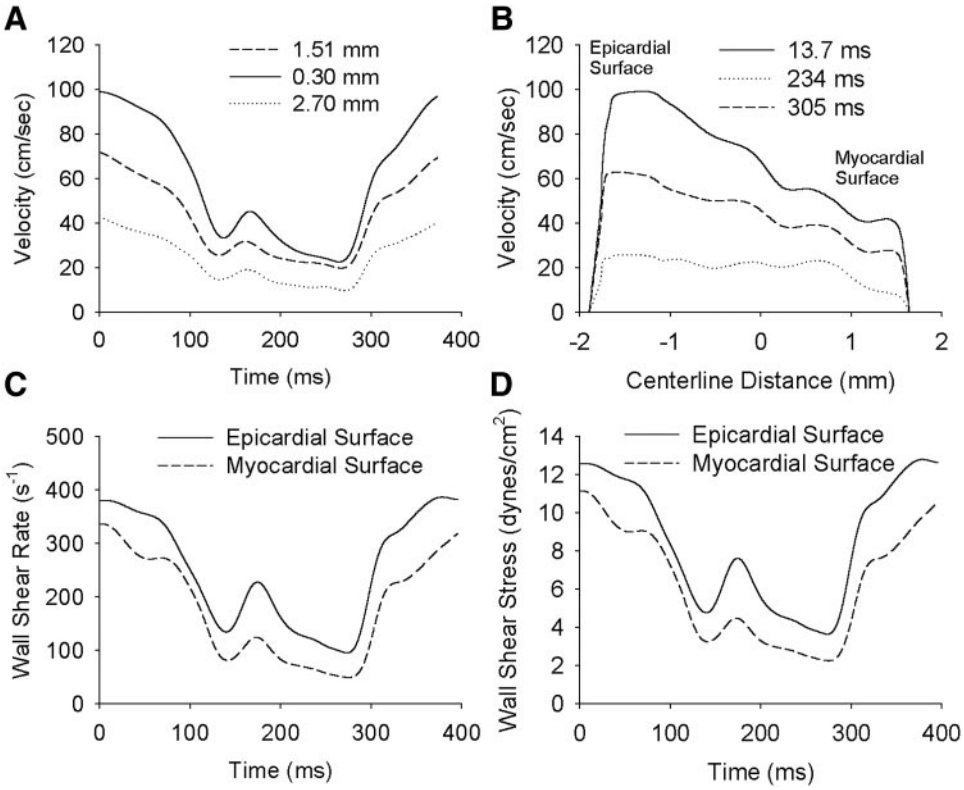

Fig. 3. Methods of LAD velocity profile and local wall shear stress estimation. *A*: ensemble-averaged LAD blood flow velocity waveforms corresponding to 3 of 14 Doppler pulse propagation distances (0.30, 1.51, and 2.70 mm) normal to the vessel wall. Spatially aligning the waveforms from each propagation depth over time allows for the reconstruction of LAD blood flow velocity profiles. *B*: velocity profiles corresponding to 3 points (13.7, 234, and 305 ms) in the cardiac cycle plotted vs. centerline distance relative to the Doppler probe 0.23 mm beneath the myocardial luminal surface. *C*: temporal changes in wall shear rate vs. time at the epicardial and myocardial luminal surfaces determined by using the finite difference method. *D*: temporal alterations in wall shear stress vs. time at the epicardial and myocardial luminal surfaces calculated as the product of shear rate and the measured in vivo viscosity.

formed (20) to acquire near wall velocity, assuming no slip at the vessel wall. Wall shear rate (γ_u) was also calculated by using a finite difference method that allowed determination of localized estimations from blood flow velocity measurements at the epicardial and myocardial luminal surfaces of the LAD proximal and distal to the implanted stent by using the differential equation $\gamma_u = -\partial u/\partial r$, where $\partial u/\partial r$ is the partial derivative of the velocity magnitude with respect to the radial position (r) (Fig. 3*C*) (6).

Determination of regional and local shear stress. Regional (τ) and local shear stress (τ_u; Fig. 3*D*) for each time point in the cardiac cycle were calculated as the product of the measured in vivo viscosity and the regional or local shear rate. Oscillatory shear stress (τ_{os}) was determined as the magnitude of the τ waveform. The rate of oscillatory shear stress ($\dot{\tau}_{os}$) was calculated as the product of τ_{os} and heart rate.

Statistical analysis. Statistical analysis of data within and between groups was conducted by using multiple ANOVA for repeated measures followed by application of Student-Newman-Keuls test. Changes within and between groups were considered statistically significant when $P < 0.05$. All data are expressed as means ± SE.

RESULTS

The systemic and coronary hemodynamic effects of adenosine in the absence and presence of an endovascular stent are summarized in Table 1. Temporal al-

Table 1. *Systemic and coronary hemodynamics*

	Baseline	Adenosine	Stent	Stent + Adenosine
HR, beats/min	138 ± 7	120 ± 10*	140 ± 10	116 ± 12*§
MAP, mmHg	114 ± 5	81 ± 5*	110 ± 2	73 ± 2*§
LVSP, mmHg	123 ± 6	90 ± 6*	119 ± 4	83 ± 4*†§
LVEDP, mmHg	9 ± 1	9 ± 1	8 ± 1	8 ± 1
LV + dP/dt_{max}, mmHg/s	1569 ± 61	1325 ± 58*	1603 ± 107	1196 ± 113*§
DCBF, ml/min	59 ± 4	189 ± 4*	77 ± 4*	162 ± 10*†§
MCBF, ml/min	34 ± 2	127 ± 9*	46 ± 4*	110 ± 11*†§
DCVR, mmHg·min^{-1}·ml^{-1}	1.95 ± 0.13	0.38 ± 0.04*	1.41 ± 0.12*	0.42 ± 0.03*§
MCVR, mmHg·min^{-1}·ml^{-1}	3.30 ± 0.16	0.61 ± 0.05*	2.70 ± 0.27*	0.77 ± 0.08*†§
PR, cP/mm^3	46 ± 3	37 ± 1*	41 ± 0*	41 ± 0*†
C, mm^3·mmHg·10^{-1}	5.09 ± 0.68	1.93 ± 0.27*	0 ± 0*	0 ± 0*†
α	2.77 ± 0.13	2.56 ± 0.04*	2.91 ± 0.12	2.64 ± 0.15§

Values are means ± SE; $n = 6$. HR, heart rate; MAP, mean arterial pressure; LVSP and LVEDP, left ventricular systolic and end-diastolic pressures, respectively; LV + dP/dt_{max}, maximum rate of increase of left ventricular pressure; DCBF and MCBF, diastolic and mean coronary blood flow, respectively; DCVR and MCVR, diastolic and mean coronary vascular resistance, respectively; PR, Poiseuillean resistance; C, LAD segmental compliance; α, Womersely number. Significantly different from *baseline, †adenosine alone, and ‡stent ($P < 0.05$).

terations in systemic and coronary hemodynamics before and after adenosine infusion and in the presence or absence of the stent are illustrated in Fig. 2. Administration of adenosine produced significant ($P < 0.05$) decreases in heart rate, mean arterial and LV systolic pressure, and maximum rate of increase of LV pressure (LV $+dP/dt_{max}$). LV end-diastolic pressure was unchanged. Increases in diastolic and mean coronary blood flows and corresponding reductions in segmental Poiseuillean and mean and diastolic coronary vascular resistance were also observed. LAD segmental compliance decreased during adenosine infusion. Adenosine increased Re (80 ± 4 to 302 ± 19), De (82 ± 5 to 310 ± 18), and Re_s (55 ± 7 to 868 ± 116) before stent implantation (Fig. 4). A decrease in α also occurred (Table 1). Increases in τ (10.7 ± 0.6 to 41.4 ± 1.5 dyn/cm^2), τ_{os} (12.4 ± 1.5 to 47.7 ± 3.6 dyn/cm^2), and $\dot{\tau}_{os}$ (1,693 ± 209 to 5,704 ± 650 dyn·cm^{-2}·min^{-1}) were observed during administration of adenosine (Fig. 5). The τ_u at the epicardial and myocardial luminal surfaces of the vessel also increased during infusion of adenosine before stent implantation (Fig. 6).

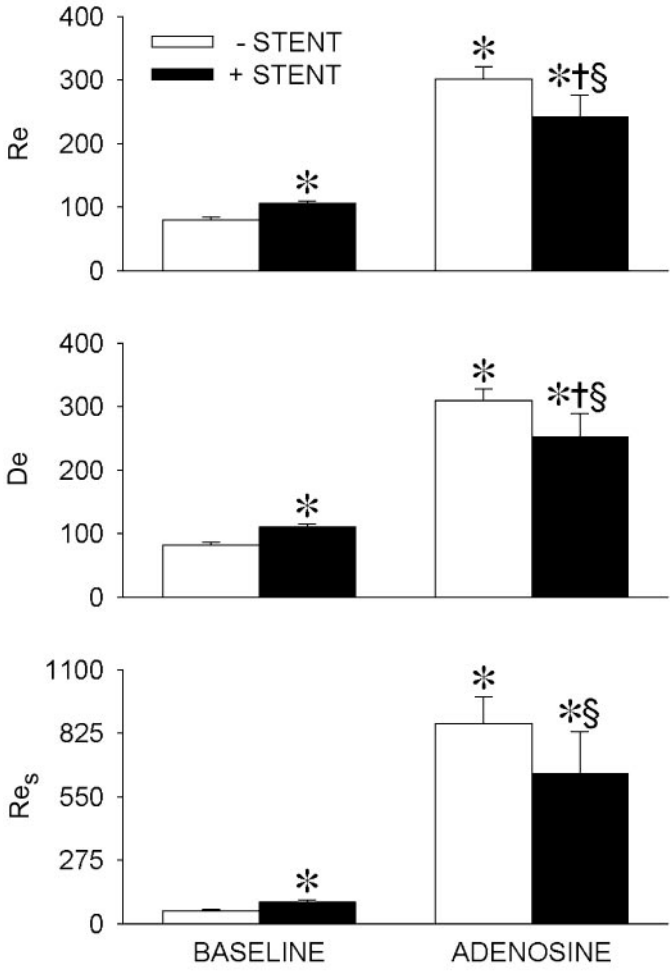

Fig. 4. Histogram depicting Reynolds number (Re; *top*), Dean number (De; *middle*), and secondary Reynolds number (Re_s; bottom) under baseline conditions and during the administration of adenosine (1.0 mg/min) in the absence (−stent; open bars) and presence (+stent; solid bars) of the intracoronary stent. Values are means ± SE. Significantly different from * −stent alone, † −stent during adenosine, and § +stent alone ($P < 0.05$).

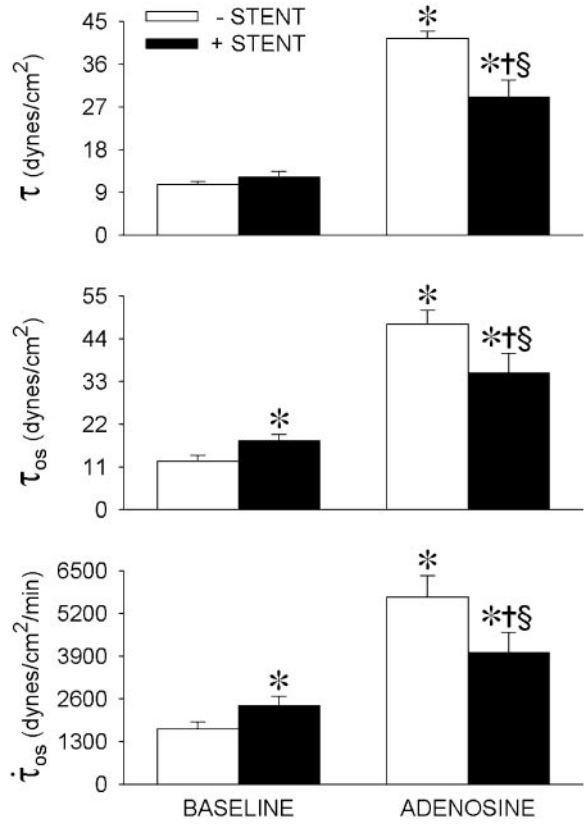

Fig. 5. Histogram depicting regional shear stress (τ; *top*), regional oscillatory shear stress (τ_{os}; *middle*), and regional oscillatory shear rate ($\dot{\tau}_{os}$; *bottom*) under baseline conditions and during the administration of adenosine (1.0 mg/min) with absence (−stent; open bars) and presence (+stent; solid bars) of the intracoronary stent. Significantly different from * −stent alone, † −stent during adenosine, and § +stent alone ($P < 0.05$).

Placement of the endovascular stent did not alter systemic hemodynamics (Table 1). Increases in coronary blood flow and reductions in mean and diastolic coronary vascular as well as segmental Poiseuillean resistance were observed after stent implantation. LAD segmental compliance was equal to zero after stent implantation. Increases in Re, De, and Re_s also occurred (Fig. 3), but α was unchanged. The τ_{os} and $\dot{\tau}_{os}$ increased after stent implantation (Fig. 5). In contrast, τ_u was unchanged immediately proximal and distal to the stent at the epicardial and myocardial luminal surfaces of the vessels.

Adenosine produced similar alterations in systemic hemodynamics in the presence and absence of the stent. Declines in heart rate, mean arterial pressure, and LV $+dP/dt_{max}$ were observed during administration of adenosine after stent placement. Adenosine-induced increases in diastolic and mean coronary blood flow concomitant with reductions in Poiseuillean and coronary vascular resistance were observed. However, the changes in these variables were attenuated in the presence of the stent. Coronary blood flow reserve was

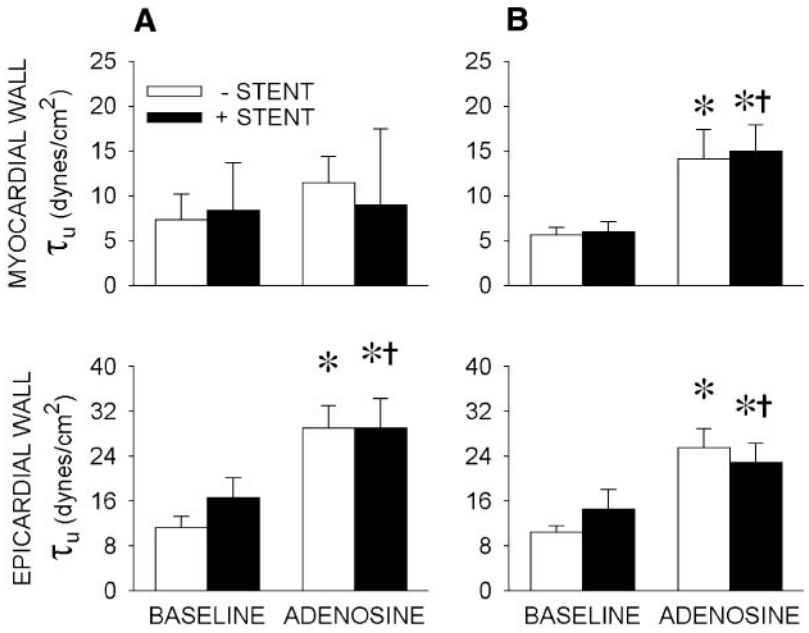

Fig. 6. Histograms depicting local shear stress (τ_u) at the proximal myocardial luminal surface (*A*, *top*), distal myocardial luminal surface (*B*, *top*), proximal epicardial luminal surface (*A*, *bottom*), and distal epicardial luminal surface (*B*, *bottom*) in the absence (−stent; open bars) and presence (+stent; solid bars) of the intracoronary stent. Significantly different from *−stent alone and †+stent alone ($P < 0.05$).

also reduced by stent implantation (144 ± 8 to 86 ± 8 ml/min). Increases in Re, De, and Re_s were observed during administration of adenosine infusion after stent implantation but were significantly lower than those observed before the stent was deployed (Fig. 4). Adenosine-induced increases in τ, τ_{os}, and $\dot{\tau}_{os}$ were also attenuated in the presence compared with the absence of the stent (Fig. 5). However, increases in τ_u proximal and distal to the stent were similar to those observed during administration of adenosine before the stent was implanted (Fig. 6). There were no differences in μ between interventions.

DISCUSSION

Intimal hyperplasia within a stented region of the coronary arteries remains a significant problem in 15–20% of patients (10, 27, 28). A number of studies have extensively examined the time course and physiological mechanisms of vessel restenosis after stent placement, but the role of changes in coronary fluid dynamics in this process has not been thoroughly investigated (9, 25). Alterations in coronary hemodynamics within the stented region may contribute to restenosis concomitant with vascular injury sustained during implantation. Tissue responses resulting from stent implantation may persist for up to 3 mo after the intervention (28) and vary with stent type (14). In addition, recent evidence suggests that τ_u distributions during this time may influence vascular smooth muscle cell response to the sustained vascular injury (18). The geometry of the involved vessel is an important factor that influences shear stress distributions (21), and regions of maximal intimal thickening have been strongly correlated with areas of low wall shear stress and deviations of the principal τ_u vector from the prominent flow direction in other arterial vascular beds (16). Intimal hyperplasia has also been shown to occur in regions of low shear stress proximal and distal to a stent (13), suggesting that altered shear stress distributions may contribute to restenosis in these areas after stent deployment (5, 33). The impedance mismatch between an implanted stent and the native artery may lead to secondary flow and contribute to neointimal hyperplasia (5). Stent implantation likely causes alterations in spatial and temporal wall shear stress gradients, which have been associated with altered membrane fluidity and proliferation in isolated endothelial cells (2, 7). Taken as a whole, these data support the hypothesis that changes in fluid dynamics due to stent geometry may be risk factors for restenosis. Importantly, studies conducted to date have evaluated the impact of stents on fluid dynamics under steady-state conditions but not during increases in blood flow resulting from exercise or exogenously administered vasodilators.

This is the first study to investigate the role of changes in coronary fluid dynamics during vasodilation in the presence and absence of a coronary stent. The present results indicate that stent implantation produces a modest increase in coronary blood flow concomitant with a reduction in coronary vascular resistance. Increases in regional wall shear stress and wall τ_{os} observed after stent placement can be attributed to the increase in coronary blood flow because viscosity was constant for the duration of the experiments. Regulation of coronary artery blood flow occurs at the arteriolar level under normal conditions. Mechanical stimulation of the normal endothelial barrier during stent implantation may have produced modest coronary vasodilation by a nitric oxide-mediated mechanism (30) or by prostacyclin release (8) by remnant endothelial cells, resulting in increases in coronary blood flow and shear stress. Increases in Re, De, and Re_s indicate that blood flow in the LAD remains lami-

nar after stent implantation but that secondary flow could be potentiated.

The present results also indicate that stent implantation alters the fluid dynamic responses of the coronary artery to pronounced vasodilation. Adenosine-induced reductions in coronary vascular resistance and increases in Re, De, and indexes of τ were attenuated after the stent was deployed. Re and De were lower in the presence of adenosine after stent implantation, suggesting that the stent attenuated skewing of the laminar axial velocity profile toward the epicardial luminal surface of the vessel and reduced secondary flow at the myocardial wall, an observation that was occasionally noticed during velocity profile reconstruction after stent implantation. Interestingly, the magnitude of adenosine-induced LAD coronary blood flow velocity waveforms proximal and distal to the stent was less pronounced and contained more transients during end diastole than those in the absence of the stent (Fig. 2), suggesting that the impedance mismatch between the implanted stent and native artery may be maximized during pronounced vasodilation and that the transients in these waveforms may be due to reflected waves or secondary flow within the stented region of the vessel. In contrast, adenosine-induced increases in Re_s were similar after stent placement, implying that increases in secondary flow during profound coronary vasodilation were similar in the absence and presence of the stent. Attenuation of indexes of τ after stent implantation during administration of adenosine suggests that the stent partially inhibits flow within this region of the vessel, resulting in localized regions of low shear stress that may potentially increase particle residence time, contribute to vascular smooth muscle cell migration and proliferation, and induce intimal hyperplasia (9, 18, 32). This hypothesis remains to be tested. The results further indicate that coronary blood flow reserve is also attenuated in the presence of a stent. Increases in coronary flow reserve after placement of coil or slotted-tube stents have been previously described in patients with coronary artery stenoses (29). However, the present results in dogs with normal coronary arteries suggest that the presence of a slotted-tube stent impedes coronary compliance within this vascular segment. This paradox is likely due to the difference between placing a stent in a healthy vessel as opposed to a calcified vessel and elucidates changes in the mechanical properties within this vascular segment after stent implantation.

Adenosine infusion resulted in decreased Poiseuillean resistance and compliance within the stented region before stent implantation. Similarly, Poiseuillean resistance within this region decreased after stent implantation but was greater than during the adenosine intervention before stent implantation. Also, the compliance of the stented region was effectively reduced to zero after stent implantation in the presence or absence of adenosine (Table 1, Fig. 2). These results suggest that hemodynamic alterations secondary to resistance and compliance differences (i.e., impedance mismatch) between stented and native regions of the LAD may depend on the ability of the stented vessel to dilate, a vascular property that is limited by the mechanical and geometric characteristics of the stent.

The findings of this investigation demonstrate that adenosine-induced alterations in τ_u at the epicardial and myocardial surfaces proximal and distal to the stent were unchanged after the stent was deployed. These findings contrast to some degree with the results of computational models and flow visualization studies (4, 5, 23, 32, 33). The Doppler method used in the present investigation has been previously utilized to resolve differences in shear stress between the epicardial and myocardial luminal surfaces (3), but its efficacy in assessing τ_u distributions immediately proximal and distal to the stented region of a coronary artery has not been specifically evaluated.

The present results should be interpreted within the constraints of several potential limitations. Stent implantation was performed in a retrograde fashion through a snared, small distal branch of the LAD. This technique clearly differs from the antegrade introduction of coronary stents used in the cardiac catheterization laboratory and was used to minimize the extent of vascular injury associated with stent placement. However, the ligation of this small LAD branch may have affected regional coronary perfusion to some degree by producing ischemia in an area of myocardium adjacent to the stent. Nevertheless, the LAD branch remained ligated before and after stent placement, and the coronary vascular response to adenosine should not have been differentially affected by this technique. Adenosine produced decreases in heart rate, mean arterial and LV systolic pressure and $+dP/dt_{max}$ of similar magnitude before and after stent placement. However, coronary perfusion pressure remained well within the autoregulatory range, and adenosine-induced increases in coronary blood flow observed here in normal coronary arteries were similar to those previously observed when arterial pressure was restored to baseline values by using partial aortic occlusion (12). Thus it is unlikely that differences in indexes of fluid dynamics between stented and normal coronary arteries during administration of adenosine were related to differential actions on systemic hemodynamics. The present results were obtained in acutely instrumented healthy dogs, and it is likely that differences in shear stress distributions observed in response to adenosine after stent implantation may be temporally affected as a result of progressive endothelialization of a chronically implanted stent and coronary artery disease. The present investigation was conducted by using a slotted-tube stent, and changes in adenosine-induced coronary flow dynamics that occur with other stent geometries cannot be directly inferred from the present results. However, it would appear likely that other types of stents with similar thickness, stent-to-artery ratios, and radial strength properties might yield similar findings. Nevertheless, the impact of various stent designs on local flow disturbances requires further investigation.

In summary, this investigation indicates that slotted-tube stent implantation attenuates alterations in coronary fluid dynamics produced by adenosine in an acutely instrumented canine model. These results may be due in part to impedance mismatching between stented and adjacent nonstented regions, as well as alterations in τ_u caused by stent implantation. Improved stent designs aimed at minimizing flow disturbances may lead to reduced vascular injury, improved stent performance, and ultimately lower rates of restenosis.

The authors thank John P. Tessmer, John G. Krolikowski, David A. Schwabe (Research Scientists, Department of Anesthesiology, Medical College of Wisconsin, Milwaukee, WI), and Shannon Timm (Research Technician, Boston Scientific-SciMed, Maple Grove, MN) for technical assistance.

This work was supported in part by Boston Scientific-SciMed and by National Institutes of Health Grants HL-03690 (to J. R. Kersten), HL-63705 (to J. R. Kersten), HL-54820 (to D. C. Warltier), GM-08377 (to D. C. Warltier), and AA-12331 (to P. S. Pagel).

REFERENCES

1. **Altobelli SA and Nerem RM.** An experimental study of coronary artery fluid mechanics. *J Biomech Eng* 107: 16–23, 1985.
2. **Bao X, Lu C, and Frangos JA.** Mechanism of temporal gradients in shear-induced ERK1/2 activation and proliferation in endothelial cells. *Am J Physiol Heart Circ Physiol* 281: H22–H29, 2001.
3. **Bell DR, Sabbah HN, and Stein PD.** Profiles of velocity in coronary arteries of dogs indicate lower shear rate along inner arterial curvature. *Arteriosclerosis* 9: 167–175, 1989.
4. **Berry JL, Moore JE, Newman VS, and Routh WD.** In vitro flow visualization in stented arterial segments. *J Vasc Invest* 3: 63–68, 1997.
5. **Berry JL, Santamarina A, Moore JE, Roychowdhury S, and Routh WD.** Experimental and computational flow evaluation of coronary stents. *Ann Biomed Eng* 28: 386–398, 2000.
6. **Bird BR, Stewart WE, and Lightfoot EN.** *Transport Phenomena*. New York: Wiley, 1960.
7. **Butler PJ, Norwich G, Weinbaum S, and Chien S.** Shear stress induces a time- and position-dependent increase in endothelial cell membrane fluidity. *Am J Physiol Cell Physiol* 280: C962–C969, 2001.
8. **Davies PF.** Flow-mediated endothelial mechanotransduction. *Physiol Rev* 75: 519–560, 1995.
9. **Edelman ER and Rogers C.** Pathobiologic responses to stenting. *Am J Cardiol* 81: 4E–6E, 1998.
10. **Fischman DL, Leon MB, Bim DS, Schatz RA, Savage MP, Penn I, Detre K, Veltri L, Ricci D, Nobuyoshi N, Cleman M, Heuser R, Almond D, Teirstein PS, Fish RD, Colombo A, Brinker J, Moses J, Shaknovitch A, Hirshfeld J, Bailey S, Ellis S, Rake S, and Goldberg S.** A randomized comparison of coronary-stent placement and balloon angioplasty in the treatment of coronary artery disease. Stent restenosis study investigators. *N Engl J Med* 331: 496–501, 1994.
11. **Garasic JM, Edelman ER, Squire JC, Seifert P, Williams MS, and Rogers C.** Stent and artery geometry determine intimal thickening independent of arterial injury. *Circulation* 101: 812–818, 2000.
12. **Hartman JC, Kampine JP, Schmeling WT, and Warltier DC.** Steal-prone coronary circulation in chronically instrumented dogs: isoflurane versus adenosine. *Anesthesiology* 74: 744–756, 1991.
13. **Hoffmann R, Mintz GS, Dussaillant GR, Popma JJ, Pichard AD, Satler LF, Kent KM, Griffin J, and Leon MB.** Patterns and mechanisms of in-stent restenosis. A serial intravascular ultrasound study. *Circulation* 94: 1247–1254, 1996.
14. **Kastrati A, Mehilli J, Dirschinger J, Pache J, Ulm K, Schuhlen H, Seyfarth M, Schmitt C, Blasini R, Neumann FJ, and Schomig A.** Restenosis after coronary placement of various stent types. *Am J Cardiol* 87: 34–39, 2001.
15. **Ku DN.** Blood flow in arteries. *Annu Rev Fluid Mech* 29: 399–434, 1997.
16. **Ku DN, Giddens DP, Zarins CK, and Glagov S.** Pulsatile flow and atherosclerosis in the human carotid bifurcation. Positive correlation between plaque location and low oscillating shear stress. *Arteriosclerosis* 5: 293–302, 1985.
17. **Lambert J, Smulders RA, Aarsen M, Gallay FP, and Stehouwer CD.** The acute effect of hyperglycemia on vessel wall properties. *Scand J Clin Lab Invest* 57: 409–414, 1997.
18. **Liu SQ and Goldman J.** Role of blood shear stress in the regulation of vascular smooth muscle cell migration. *IEEE Trans Biomed Eng* 48: 474–483, 2001.
19. **Lyne WH.** Unsteady viscous flow in a curved pipe. *J Fluid Mech* 45: 13–31, 1971.
20. **Markou CP and Ku DN.** Accuracy of velocity and shear rate measurements using pulsed Doppler ultrasound: a comparison of signal analysis techniques. *Ultrasound Med Biol* 17: 803–814, 1991.
21. **Myers JG, Moore JA, Ojha M, Johnston KW, and Ethier CR.** Factors influencing blood flow patterns in the human right coronary artery. *Ann Biomed Eng* 29: 109–120, 2001.
22. **Nichols WW and O'Rourke MF.** *McDonald's Blood Flow in Arteries: Theoretical, Experimental and Clinical Principles*. New York: Oxford University Press, 1998.
23. **Peacock J, Hankins S, Jones T, and Lutz R.** Flow instabilities induced by coronary artery stents: assessment with an in vitro pulse duplicator. *J Biomech* 28: 17–26, 1995.
24. **Pijls NH, Van Gelder B, Van der Voort P, Peels K, Bracke F, Bonnier H, and El Gamal M.** Fractional flow reserve: a useful index to evaluate the influence of an epicardial coronary stenosis on myocardial blood flow. *Circulation* 92: 3183–3193, 1995.
25. **Rogers C, Welt FG, Karnovsky MJ, and Edelman ER.** Monocyte recruitment and neointimal hyperplasia in rabbits. Coupled inhibitory effects of heparin. *Arterioscler Thromb Vasc Biol* 16: 1312–1318, 1996.
26. **Schatz RA, Palmaz JC, Tio FO, Garcia F, Garcia O, and Reuter SR.** Balloon-expandable intracoronary stents in the adult dog. *Circulation* 76: 450–457, 1987.
27. **Serruys PW, De Jaegere P, Kiemeneij F, Macaya C, Rutsch W, Heyndrickx G, Emanuelsson H, Marco J, Legrand V, Materne P, et al.** A comparison of balloon-expandible-stent implantation with balloon angioplasty in patients with coronary artery disease. Benestent study group. *N Engl J Med* 331: 489–495, 1994.
28. **Van Beusekom HM, Whelan DM, Hofma SH, Krabbendam SC, van Hinsbergh VW, Verdouw PD, and van der Giessen WJ.** Long-term endothelial dysfunction is more pronounced after stenting than after balloon angioplasty in porcine coronary arteries. *J Am Coll Cardiol* 32: 1109–1117, 1998.
29. **Vrints CJ, Claeys MJ, Bosmans J, Conraads V, and Snoeck JP.** Effect of stenting on coronary flow velocity reserve: comparison of coil and tubular stents. *Heart* 82: 465–470, 1999.
30. **Vural KM and Bayazit M.** Nitric oxide: implications for vascular and endovascular surgery. *Eur J Vasc Endovasc Surg* 22: 285–293, 2001.
31. **Warltier DC, Gross GJ, and Brooks HL.** Pharmacologic- vs. ischemia-induced coronary artery vasodilation. *Am J Physiol Heart Circ Physiol* 240: H767–H774, 1981.
32. **Wentzel JJ, Krams R, Schuurbiers JCH, Oomen JA, Kloet J, van der Giessen WJ, Serruys PW, and Slager CJ.** Relationship between neointimal thickness and shear stress after wall stent implantation in human coronary arteries. *Circulation* 103: 1740–1745, 2001.
33. **Wentzel JJ, Whelan DM, van der Giessen WJ, van Beusekom HM, Andhyiswara I, Serruys PW, Slager CJ, and Krams R.** Coronary stent implantation changes 3-D vessel geometry and 3-D shear stress distribution. *J Biomech* 33: 1287–1295, 2000.